

PARP-1 to the Rescue:
A Biphasic Mechanism of UVB-Induced DNA Damage and Repair in Cultured Human Lens
Epithelial Cells

Submitted by
Caroline S. Cencer
Biology

To
The Honors College
Oakland University

In partial fulfillment of the
requirement to graduate from
The Honors College

Mentor:
Dr. Frank Giblin, Director
Eye Research Institute
Oakland University

March 1, 2016

Abstract

It has been shown that UVB light damages the DNA of cells; however, it has yet to be shown how this occurs in lens epithelial cells (LECs) found on the anterior surface of the eye's lens. The purpose of this research project was to explore UVB-induced DNA damage to LECs along with investigation of a related DNA repair complex. A DNA repair process for LECs is hypothesized to involve two components referred to as poly(ADP-ribose) polymerase-1 (PARP-1) and poly(ADP-ribose) (PAR). The exact mechanisms for UVB induced DNA damage and its repair are not yet confirmed. To study these two events, cultured human LECs were exposed to UVB light and then incubated for various times after UVB exposure. Various assays were conducted to visualize the processes of DNA damage and repair. These assays included cell viability (MTT assay), the comet assay to detect single strand DNA breaks, reactive oxygen species (ROS) and superoxide anion indicators, as well as fluorescence immunocytochemistry with antibodies to PARP-1 and PAR and apoptosis detection. The goal was to discover how the lens DNA repair complex works in response to UVB induced cellular damage. The benefits of this project include a contribution to existing eye and cataract research.

Introduction

The lens is an essential part of vision. It sits behind the cornea and is responsible for focusing incoming light onto the retina. In order for the optimum transfer of light onto the retina's photoreceptors the lens must be perfectly transparent. With aging, however, the lens will lose soluble protein, diminishing transparency. An additional problem is the development of premature cataracts that are due to other effects besides aging. A cataract can be defined as opacity in the lens which is caused by breakdown of structural crystallines in the lens fibers. Cataract formation can also be attributed to damage of lens epithelial cells (LECs). These cells

never divide and exist on the anterior surface in the cortex region of the lens which surrounds the lens nucleus (Fig. 1). One common form of cataract is called the cortical cataract which occurs in this cortex area and leads to cloudiness in peripheral vision as well as central vision if it is within the optical axis (Jaffe & Horwitz, 1992). Research on early cataract formation and its possible causes has increased in specificity over time. One of the earlier articles written on this topic is about a study that was done on fishermen in 1988 to investigate the effect of ultraviolet (UV) radiation on the lens. In the end, it was concluded that there is a relationship between UVB radiation and cortical cataract formation (Taylor et al., 1988). Furthermore, it was discovered through a phenomenon known as the Coroneo effect that incoming UV light is 20x as damaging when entering the corner of the lens (Coroneo, 2011). Along with UVB associated DNA damage, cells also have a DNA repair mechanism in place to fix this deterioration. It comes from a family of enzymes known as poly(ADP-ribose) polymerases (PARPs) with one specific enzyme in mind known as PARP-1. The mechanism of DNA repair by PARP-1 is still a relatively unknown topic, especially when it comes to LECs. It is hypothesized that PARP-1 is activated in times of cellular stress or damage to catalyze NAD⁺ degradation into nicotinamide and ADP-ribose. This leads to the formation of poly(ADP-ribose) polymers (PAR) which then work with PARP-1 to repair the DNA. However, as helpful as PARP-1 sounds when it comes to repairing cell DNA, it is also hypothesized to induce a mechanism known as parthanatos. This is a relatively new topic concerning the negative effects of overactive PARP-1 and a surplus of PAR production. In general, parthanatos is said to happen when excess PAR polymers trigger the mitochondria to release an apoptosis-inducing factor (AIF) that translocates to the nucleus and causes cells to commit to dying (Fatokun et al., 2014). The goal of this project was to explore

UVB-induced DNA damage and PARP-1/PAR DNA repair in cultured human lens epithelial cells along with the possibility of cell death via the parthanatos mechanism.

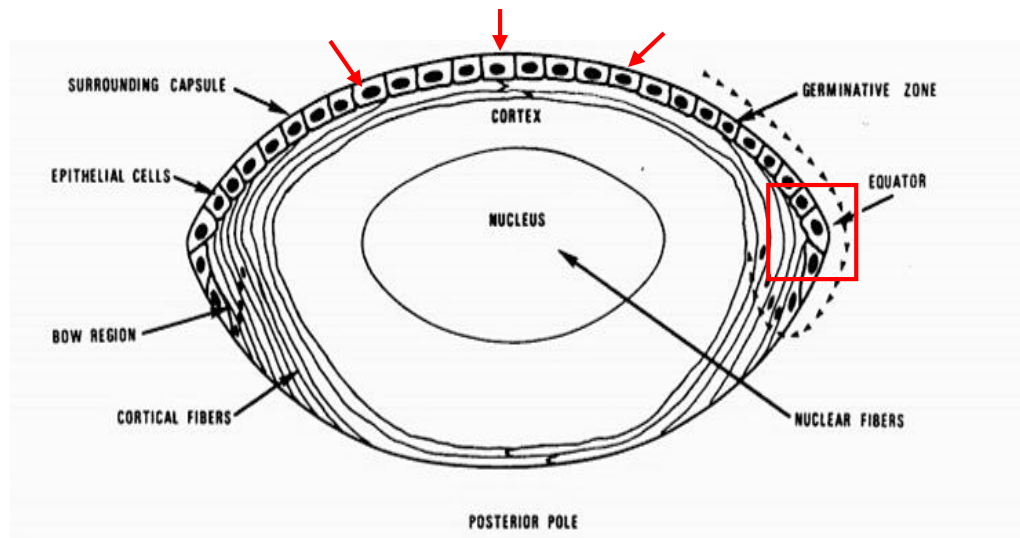


Figure 1: Diagram of the human lens showing the cortex region where lens epithelial cells (red arrows) are localized and affected by incoming ultraviolet light. LECs located at the side region (red square) are the most susceptible to UV damage to DNA due to the Coroneo effect.

Aims

1. To assess the amount of damage associated with the exposure of lens epithelial cells to UVB radiation.
2. To examine the mechanism of DNA repair by the PARP-1 enzyme and PAR polymers.
3. To understand apoptosis/parthanatos activation by excessive PARP-1 activity.
4. To compare the results of both UVB damage analysis and PARP-1 activation experiments in order to complete the hypothesized mechanism.

Objectives

1. Looking at the damage done to LECs in relation to various incubation times after UVB exposure provides a foundation for the entire project by confirming that excessive UVB radiation can lead to lens cell death.

2. Immunocytochemistry staining of the PARP-1 enzyme, PAR polymers, as well as staining for apoptosis will lead to a proposed mechanism for UVB induced DNA damage in LECs.
3. Apoptosis and reactive oxygen species (ROS) tracking will help further understand how LECs are damaged by UVB and/or parthanatos.
4. Putting the results together will generate an explanation for the process of UVB induced DNA damage and PARP-1/PAR repair in the human lens.

Methods

Culturing human LECs:

For the following experiments, the cultured human lens epithelial cells (LECs) originated from an immortalized cell line of SRA 01/04 established in 1998 at Oakland University's Eye Research Institute by Dr. Venkat Reddy (Ibaraki et al, 1998). The cells were grown in DMEM low glucose medium containing 15% Fetal Bovine Serum (FBS), Gentamicin, and Fungizone® at 37°C to confluence. Cells were then trypsinized and passaged onto 60mm plates (800,000 cells/plate), 4-well chamber slides (50,000 cells/well), or 96-well plates (10,000 cells/well).

UVB Exposure:

Before UVB exposure cells were incubated in 1% FBS medium for 1 hour followed by serum free medium for 30 minutes. They were then washed in phosphate buffered saline (PBS) and placed onto the UVB setup (Fig. 2). The UV lamp had a wavelength range of 270-380nm with a 312nm peak. The cell plates were placed on top of a UVC filter with the UV lamp underneath. This ensured that UVC light was not a factor interacting with the cells. After a 2.5 minute UVB exposure at an intensity of 0.9mW/cm² and a fluence of 0.14J/cm², the cells were incubated at 37°C for various time points.

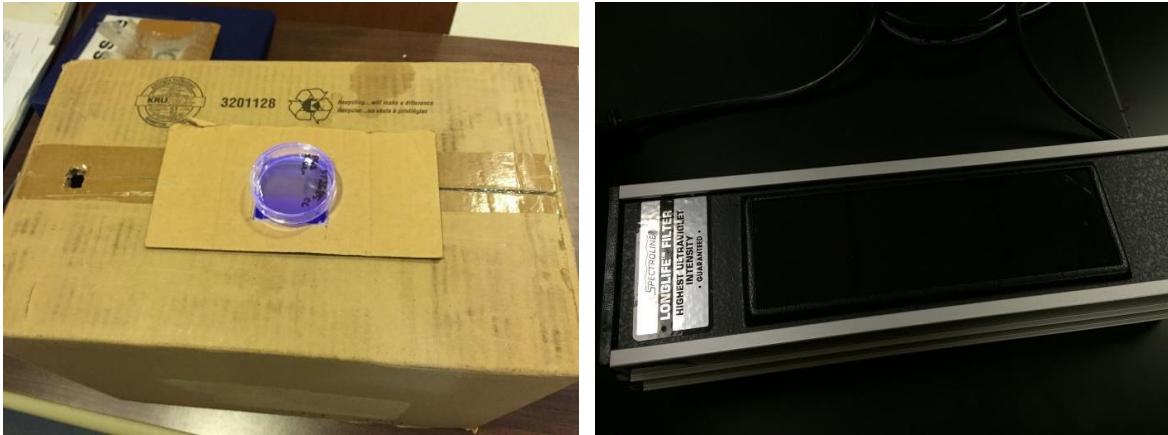


Figure 2: UVB lamp set up for exposing LECs for experimentation. The plate of cells sits on top of a UVC glass filter (left) which is on top of the UV lamp (right). The lamp has a peak wavelength of 312nm while the UVC filter eliminates light below 280nm. UVB light exists from 280nm-315nm.

MTT Assay:

Following UVB irradiation and various times of incubation, the 15% FBS media was removed from the wells of a 96-well plate and MTT solution was added to each well and the plates were incubated for 2 hours at 37°C. (MTT stock solution was made with 5 mg MTT/10mL serum free DMEM) After incubation, the MTT was removed and organic solvent was added to extract the dye. (27 mL Isopropanol, 3mL Triton X-100, 2.5 μ L HCl). The BioTek Epoch 2 Microplate Spectrophotometer and Gen5 Data Analysis Software were used to measure optical density (OD) units for each 96-well plate at a wavelength of 570nm.

Comet Assay:

To detect single strand DNA breaks, the comet assay was performed. Treated cells were washed twice with PBS and harvested by scraping. Harvested cells were transferred to a vial and centrifuged at 1500 RPM, 4°C for 15 minutes to form a cell pellet. The supernatant was removed and the cell pellet was re-suspended in PBS and homogenized. Irradiated cells were then mixed

with 0.5% low melting agarose (LMPA). This mixture was then placed onto 0.5% normal melting agarose (NMA) coated slides with a square cover slip. The slides were refrigerated for 5-7 minutes to allow the agarose to set and then the cover slip was carefully removed. Additionally, 0.5% LMPA was then pipetted onto the square gel. The slides were again refrigerated and the cover slip was removed. The slides were incubated for one hour at 8°C with lysing solution (2.5M NaCl, 100mM EDTA, 10mM Trizma Base, pH 10.0, and 1% Triton X-100). Next, the slides were placed into electrophoresis buffer (1mM EDTA, 300mM NaOH) for 20 minutes. Electrophoresis was run for 30 minutes at 24 volts (300mA) in the cold room. After electrophoresis, slides were neutralized in Tris base (0.4 M, pH 7.5) for 5 minutes. The cells were stained with EtBr (20mg/mL) for 5 minutes and then rinsed by dipping the slides in chilled deionized water. Glycerol was used to mount the slides and the Zeiss fluorescence microscope was used to observe the DNA fragments.

TMR Roche Red *In Situ* Cell Death Detection Kit:

For a second method of detecting DNA strand breaks, LECs were cultured onto 4 well chamber slides (50,000 cells/well) and exposed to UVB. After irradiation, the cells were fixed with 4% paraformaldehyde (PFA) for 30 minutes at room temperature. After washing with PBS, the cells were permeabilized with 0.125% Triton X-100 for 15 minutes at room temperature. The TUNEL reaction mixture was made by combining 50µL of the Enzyme Solution with 450µL of the Label Solution. This mixture was added to the wells of the chamber slide and the cells were incubated for 1 hour at 37°C in a dark, humidified environment. The cells were washed with PBS, mounted, and imaged with the Zeiss fluorescence microscope.

Reactive Oxygen Species (ROS):

Following UVB irradiation and various times of incubation, 1µl each of CellROX Red reagent and CellROX Green Reagent were added to each well of 4-well chamber slides containing 500µL 15% FBS media. The cells were incubated with the ROS reagents for 30 minutes at 37°C. After incubation, the cells were washed three times with PBS. Next, the cells were fixed in 4% paraformaldehyde (PFA) for 30 minutes at room temperature. The PFA was removed and the slides were mounted with glycerol and viewed under a Zeiss fluorescence microscope.

Superoxide Anion Indicator for Live Cells:

For detecting the oxygen free radical superoxide anion, a 5mM MitoSOX reagent stock solution was made by dissolving the contents of 1 vial (50µg) of MitoSOX mitochondrial indicator in 13µL of DMSO. This stock was then diluted in DPBS +Mg +Ca to a 1µM solution. 200µL of the diluted solution was placed into each well of the slides and the cells were incubated for 10 minutes at 37°C out of light. After incubation, the solution was removed and the cells were counterstained with Hoechst dye (1:2000) for 5 minutes in the dark. After counterstaining, the cells were washed 3 times with warmed DPBS +Mg +Ca and the slides were mounted with a small amount of the DPBS and a coverslip. Cells were imaged with the Zeiss fluorescence microscope.

Immunocytochemistry- PARP-1:

Following UVB irradiation and various times of incubation, immunocytochemistry was performed to detect PARP-1 in the LECs. Media was removed from the wells of the chamber slides and the cells were washed one time with PBS. Cells were then fixed in 4% PFA for 30

minutes at room temperature. After fixation, the cells were washed three times with PBS. Next, cells were incubated in 0.125% Triton X-100 for 15 minutes at room temperature and then washed three times with PBS. Next, 5% Normal Goat Serum (NGS) was added to the cells as blocking solution for 1 hour at room temperature. NGS was removed and primary antibody (Trevigen® Anti-PARP clone C2-10) at a 1:400 dilution was added overnight at 8°C. The next day, the primary antibody was removed and the cells were washed three times with PBS. Secondary antibody (Alexa Fluor® 568 Goat anti-Mouse) at a 1:200 dilution was added for 2 hours at room temperature. Secondary antibody was removed and the cell nuclei were stained with DAPI for 5 minutes at room temperature (1:5000). Cells were washed three times with PBS and slides were mounted with glycerol and viewed under a Zeiss fluorescence microscope.

Immunocytochemistry- PAR Polymers:

The same procedure was employed for tagging PAR polymers that is mentioned above in regards to PARP-1 staining. Instead of a PARP-1 antibody, a 1:400 dilution of Enzo® Life Sciences Poly(ADP-ribose) primary antibody was used to detect PAR.

Immunocytochemistry- AIF:

Apoptosis inducing factor (AIF) was stained with a 1:100 dilution of Cell Signaling Technology® AIF Antibody along with a green anti-rabbit secondary antibody. Like PARP-1 and PAR immunocytochemistry, the AIF methods differed only in the antibodies used.

Results

UVB Exposure:

In order to study the effects of UVB radiation on normal cell morphology, SRA 01/04 LECs were grown on 100mm plates for 6 days. Experimental plates were exposed to UVB for 2.5 minutes on day 1 of growth while the control plates did not come into contact with UVB. Cells were viewed with a Nikon Eclipse TS100 microscope and photos were imaged using Spot 5.2 Basic Software (Fig. 3). The control plate grew to confluence with cells tightly covering the entire surface of the plate. The control LECs did not show any signs of damage and had normal LEC morphology after 6 days as expected. The plate that was exposed to UVB prior to the growth period, however, did not come anywhere near reaching confluence after 6 days, was very sparse, and showed many morphological abnormalities that are representative of UVB-induced cell damage. These include branch-like connections between adjacent cells (arrows) as well as an abnormal, oblong shape.

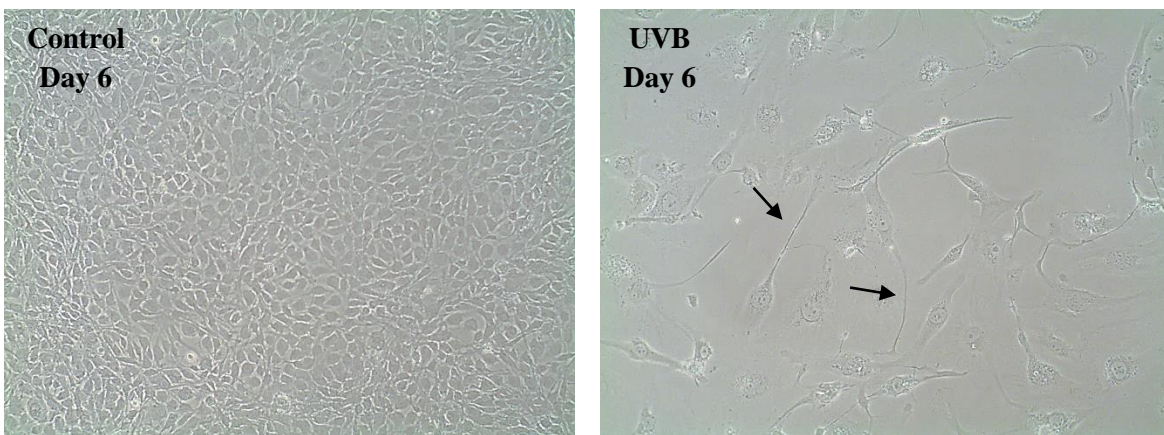


Figure 3: Images taken for LEC growth both without any UVB radiation (left) and 6 days after UVB radiation (right). The UVB plate experienced poor growth and the development of branch-like structures (arrows) while the control plate was able to grow to confluence.

MTT Cell Viability:

The MTT assay was used for assessing the concentration of live cells grown on a 96 well plate. The amount of live cells can be determined from optical density (OD) that is measured by a spectrophotometer at a specific wavelength of 570nm (Table 1). MTT solution is a mixture of the chemical Thiazolyl Blue Tetrazolium Bromide and serum free DMEM media. Live cells convert the MTT into a purple product known as formazan (Riss et al., 2013). The purple coloring is then extracted with an organic solvent. The more intense the color is, the more viable cells there are (Fig. 4). Absorbance readings given by the spectrophotometer at 570nm can be evaluated to determine how cells are affected by UVB radiation. These values were averaged for each time point and the percent loss of LECs were calculated from the control cells (Table 1).



Figure 4: LECs that have transformed MTT into formazan. The purple color that is produced is extracted from the cells with organic solvent. A stronger color indicates more live cells in the well. Note how the 24 hour control (left) has much more intense pigment than the 24 hour UVB exposed plate (right).

	1 hour	3 hours	24 hours	48 hours
Control	0.275±0.037	0.275±0.037	0.535±0.008	0.865±0.047
UVB-Exposed	0.202±0.014	0.196±0.033	0.158±0.034	0.176±0.082
% Loss of LECs	26%	28%	70%	80%

Table 1: Averaged optical density data for n=3 of each time point after UVB irradiation. The percent loss of cells was calculated from the respective control plate (3 hours, 24 hours, 48 hours) and the standard deviation comes from the averaged data for each time point. 24 hours and 48 hours after initial UVB exposure show the greatest amount of cell death.

Comet Assay:

The goal of the comet assay was to visualize the UVB induced damage in LECs through gel electrophoresis of DNA fragments. DNA is negatively charged due to its phosphate groups, and is pulled toward the positive terminal of the electrophoresis. Smaller fragments travel faster through the agarose gel than large fragments. Therefore, the longer the “tail” is, the more DNA damage occurred. When stained with ethidium bromide, the size of the broken DNA tails can be observed to quantify the amount of damage done by UVB after each time point of incubation. Damage to the LECs occurred instantaneously as well as after 90 minutes. Interestingly, the damage seen at 0 minutes was repaired by 30 minutes but is seen again at 90 minutes suggesting a biphasic mechanism for UVB-induced DNA damage and repair.

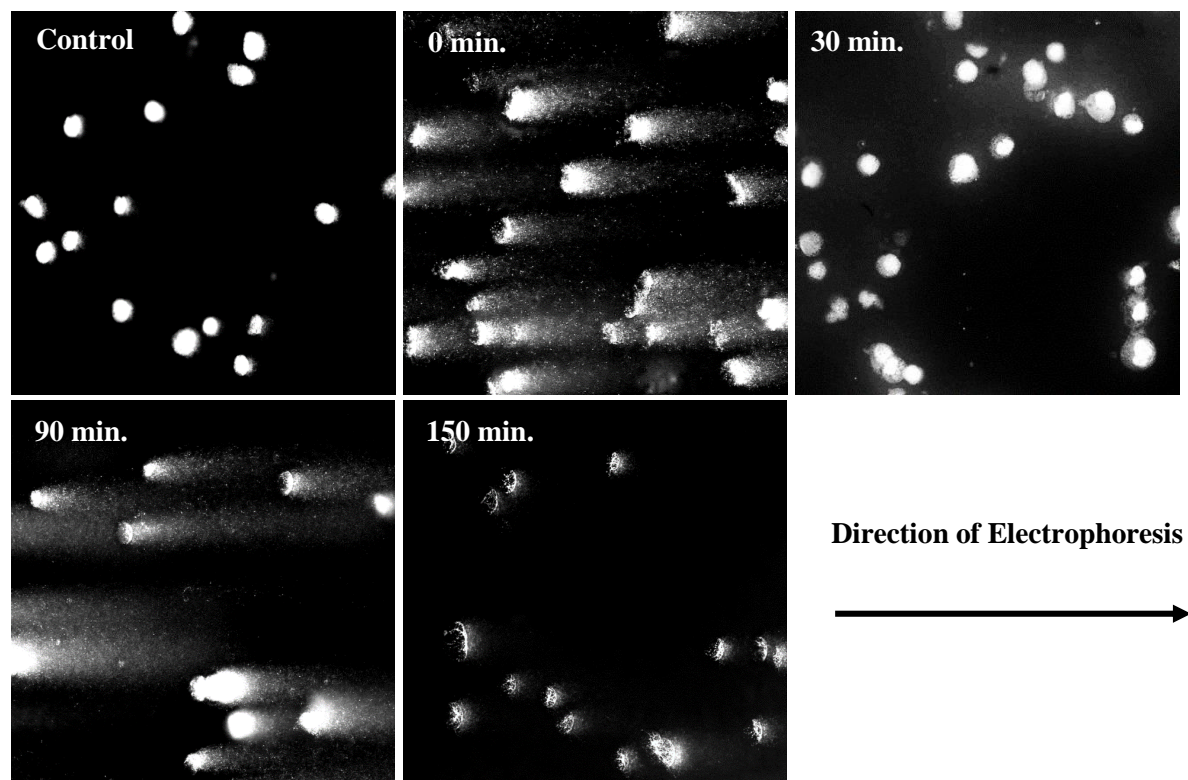


Figure 5: Visualization of DNA fragments being pulled out of LEC nuclei by electrophoresis. Note the 2 peaks of DNA damage immediately after UVB exposure as well as after 90 minutes of incubation. DNA shows repair after 30 minutes and again after 150 minutes of incubation.

TMR Roche Red:

After visualizing the damage that UVB causes human LECs, the next goal was to understand how and why there is a biphasic mechanism. We explored the process of apoptosis, programmed cell death, in response to UVB-induced DNA damage. An early study done on human lenses detected high levels of apoptotic cells in cataract patients when compared to normal lenses (Li et al., 1988). We hypothesized that part of the reason the LECs showed such dramatic cell death 24 and 48 hours after UVB treatment in the MTT assay was due to them somehow being directed toward apoptosis. The TMR red *in situ* cell death detection kit was used to locate the time of apoptosis in LECs following UVB radiation. Similar to the results of the comet assay, apoptosis was detected in the LECs both 5 minutes and 90 minutes after UVB

radiation. Yet very low levels were detected in the control, 30 minutes, 60 minutes, and 120 minutes after irradiation.

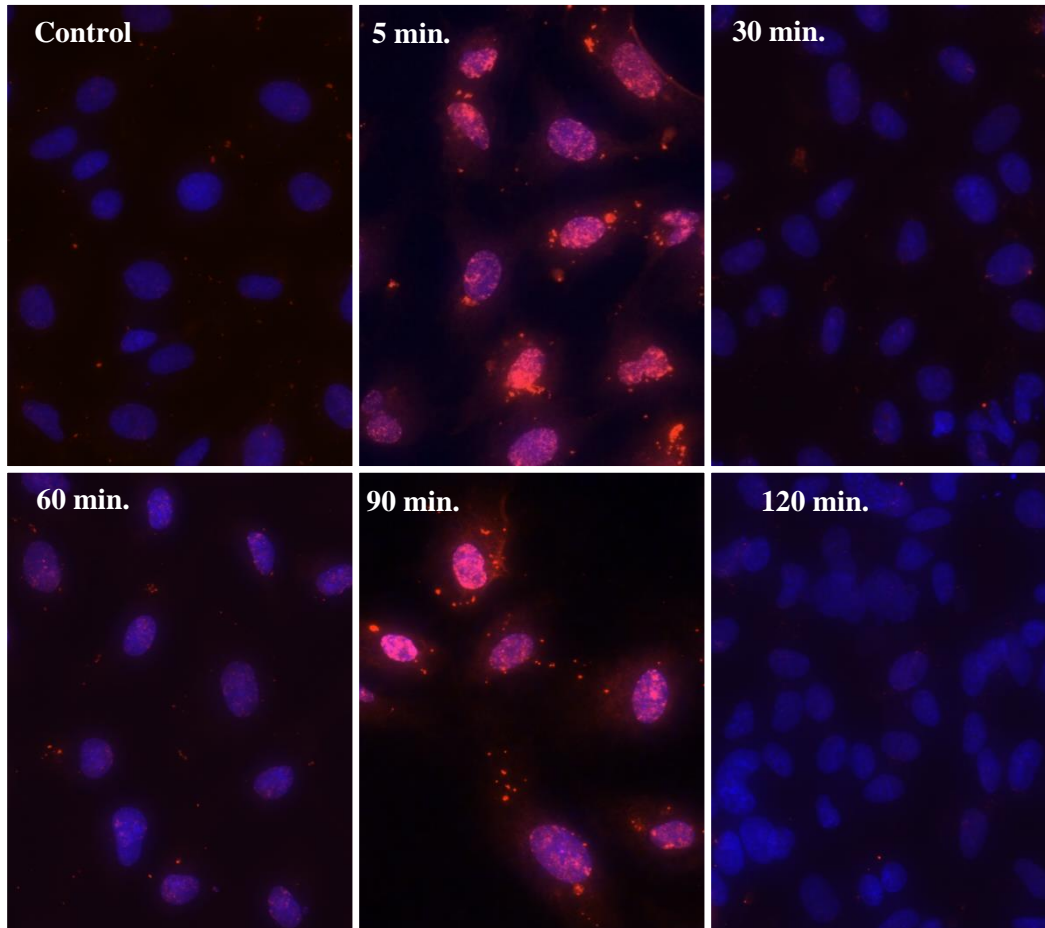


Figure 6: Apoptosis staining in irradiated LECs after various times of incubation. Blue= DAPI nuclei staining Red= apoptosis staining in cytoplasm Pink= apoptosis staining in nuclei.

ROS:

Reactive oxygen species (ROS) are molecules that develop within the cell and are known to cause oxidative damage. One example of a ROS is hydrogen peroxide, H_2O_2 . CellROX® Green and CellROX® reagents were used to see if the same held true for lens epithelial cells after UVB exposure caused DNA damage. With the reagents, ROS localized in the cytoplasm is

stained red while the ROS found in the nucleus is green. Overlap appears orange. It is important to note that ROS is mostly expressed at 90 minutes after initial UVB treatment (Fig. 7).

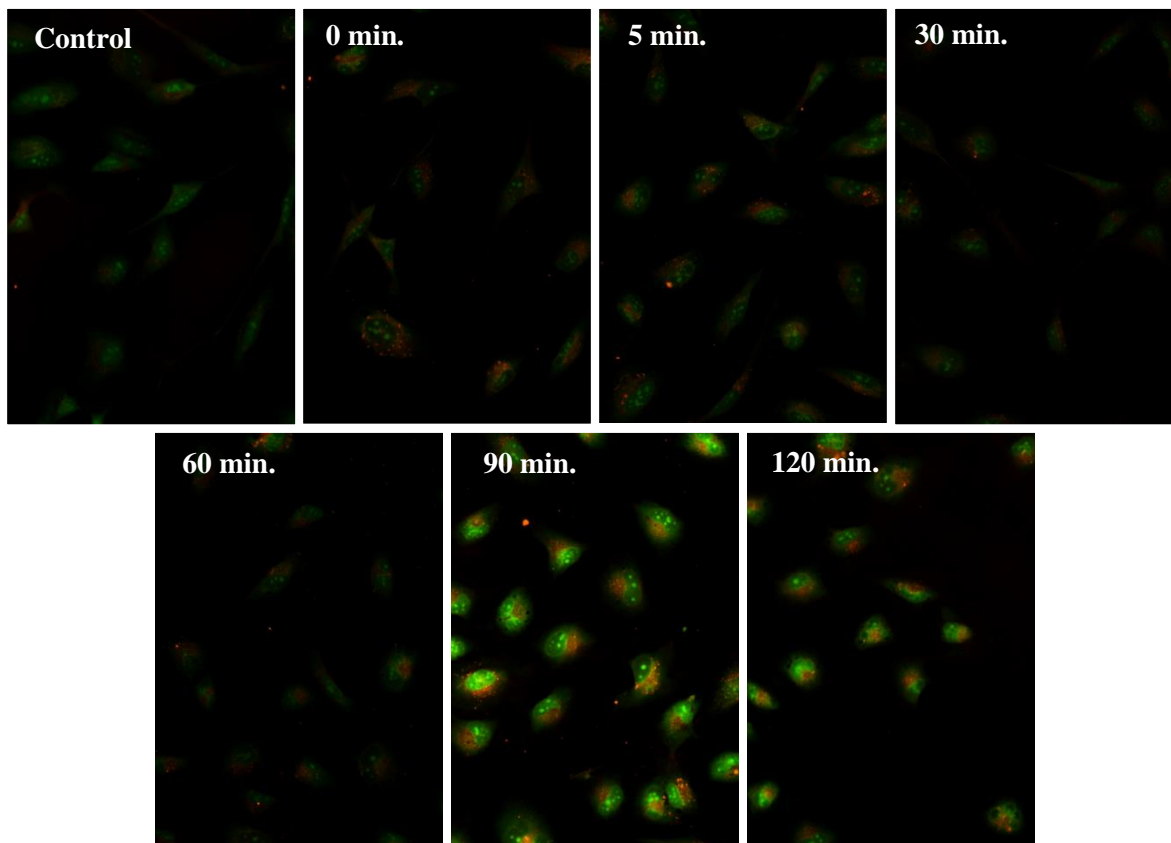


Figure 7: ROS in cytoplasm= red ROS in nucleus= green. Little H₂O₂ development is observed for the first hour. However, there is an increased production of ROS after 90 minutes of incubation which persists in the cells.

Superoxide Indicator:

As the most prominent type of ROS, superoxide anion, $\bullet\text{O}_2^-$, can have lasting harmful effects on cells. We wanted to discover if superoxide is present in LECs, when it is expressed, and where it is localized. To do this, we used the MitoSOX™ Red Mitochondrial Superoxide Indicator to detect superoxide in the mitochondria of live LECs. Chemical reduction of oxygen in the mitochondria produces superoxide which can be converted into H₂O₂ (Murphy, 2008). The

accumulation of these molecules can cause oxidative damage to DNA (Fig. 8). Superoxide was nonexistent in the cells until 90 minutes after initial UVB exposure when it is strongly expressed.

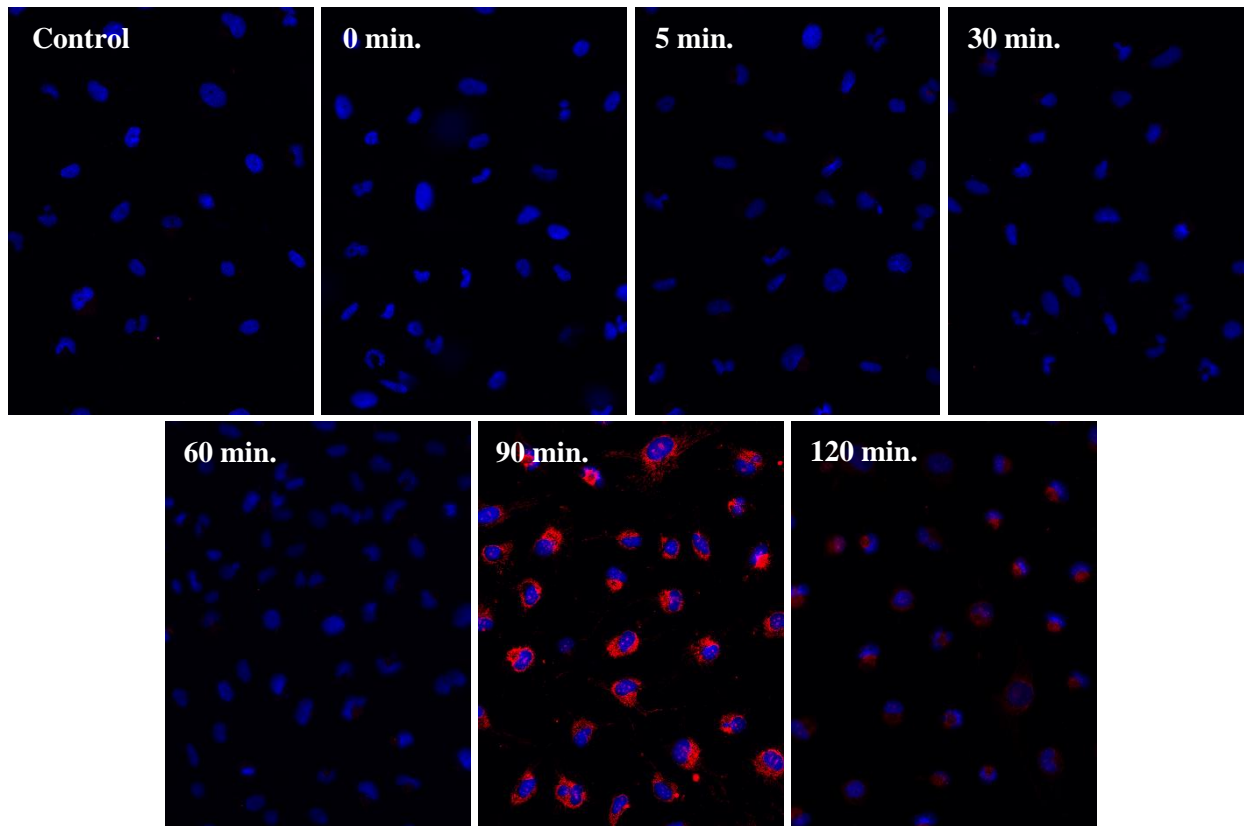


Figure 8: Superoxide anion staining in the mitochondria of irradiated LECs after various incubation times. Blue= Hoechst dye nuclei staining Red= superoxide in mitochondria. This kit is for the detection of superoxide anion in live cells.

Immunocytochemistry: PARP-1

Immunocytochemistry is a method to stain and locate specific elements in a cell. In order to understand the biphasic PARP-1 repair mechanism, we first stained for PARP-1 to see whether it was located in the nucleus or in the cytoplasm and if it only appears after UVB-induced DNA damage (Fig. 9). Immunocytochemistry works by using antibodies to tag whatever is being targeted. In this case, PARP-1 was labeled with an Anti-PARP-1 primary antibody. Then a secondary antibody was applied to add a fluorescent tag to the primary antibody so that it would fluoresce at its optimal wavelength. The level of PARP-1 was found to be constant in

LECs at all times after UVB exposure and also in the absence of UVB. The level of PARP-1 expression did not change.

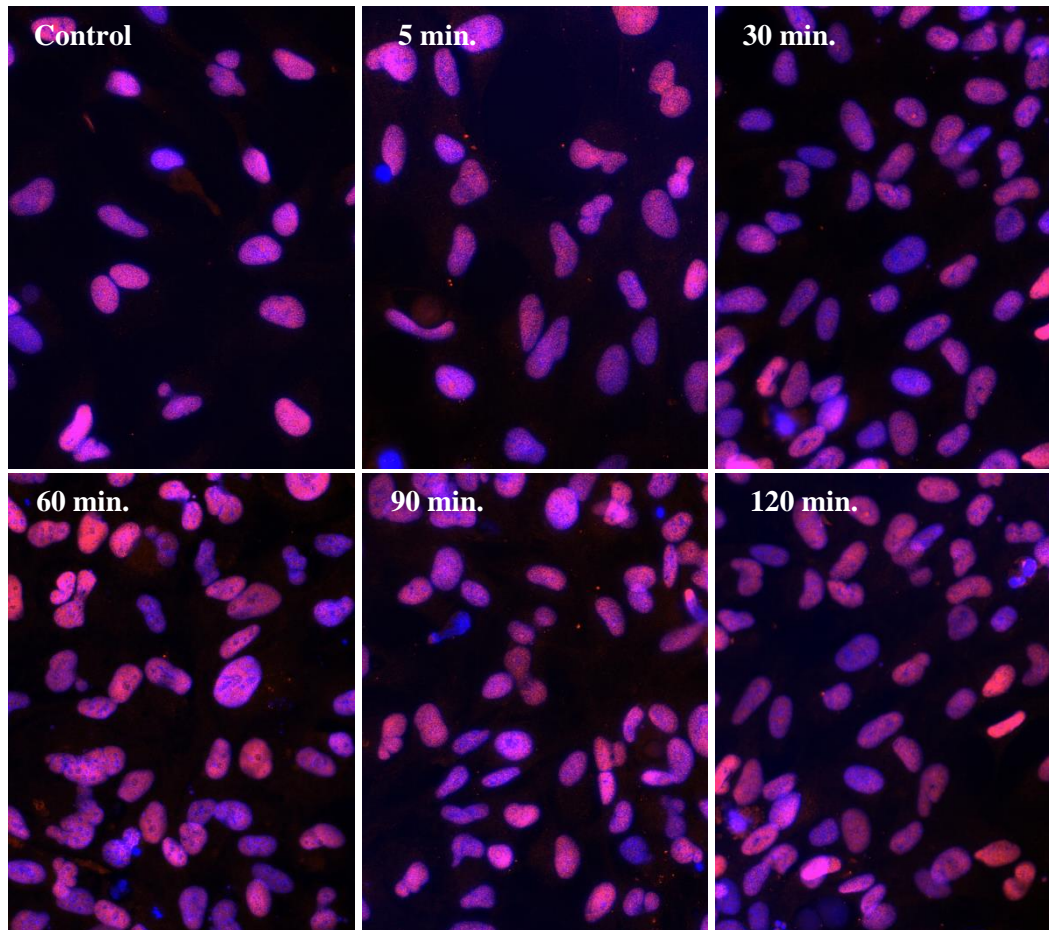


Figure 9: PARP-1 staining in irradiated LECs after various incubation times. Blue= DAPI nuclei staining Red= PARP-1 in cytoplasm Violet= PARP-1 in nucleus.

Immunocytochemistry: PAR

Recall that PARP-1 degrades NAD^+ in the cytoplasm into nicotinamide and ADP ribose elements. Then the ADP ribose units clump together to form poly(ADP-ribose), or PAR, polymers. Since immunocytochemistry with PARP-1 revealed its constant presence in the nucleus, the next question was whether or not PAR follows this same continuous pattern. However, we hypothesized that PAR would only be formed by PARP-1 during times of cell stress or DNA damage. Immunocytochemistry staining for an Anti-PAR antibody produced the

following images concerning the localization of PAR in response to UVB-induced DNA damage (Fig. 10). The protocol to detect PAR in the LECs was identical to the PARP-1 staining, but used a different primary antibody, one that tags PAR instead of PARP-1. The same secondary antibody was used and the cells were imaged in the same way. Unlike the PARP-1 results, PAR showed a dramatic fluctuation in expression. It shows a biphasic presence at both 5 minutes and 90 minutes after initial UVB exposure. PAR was not present in the control.

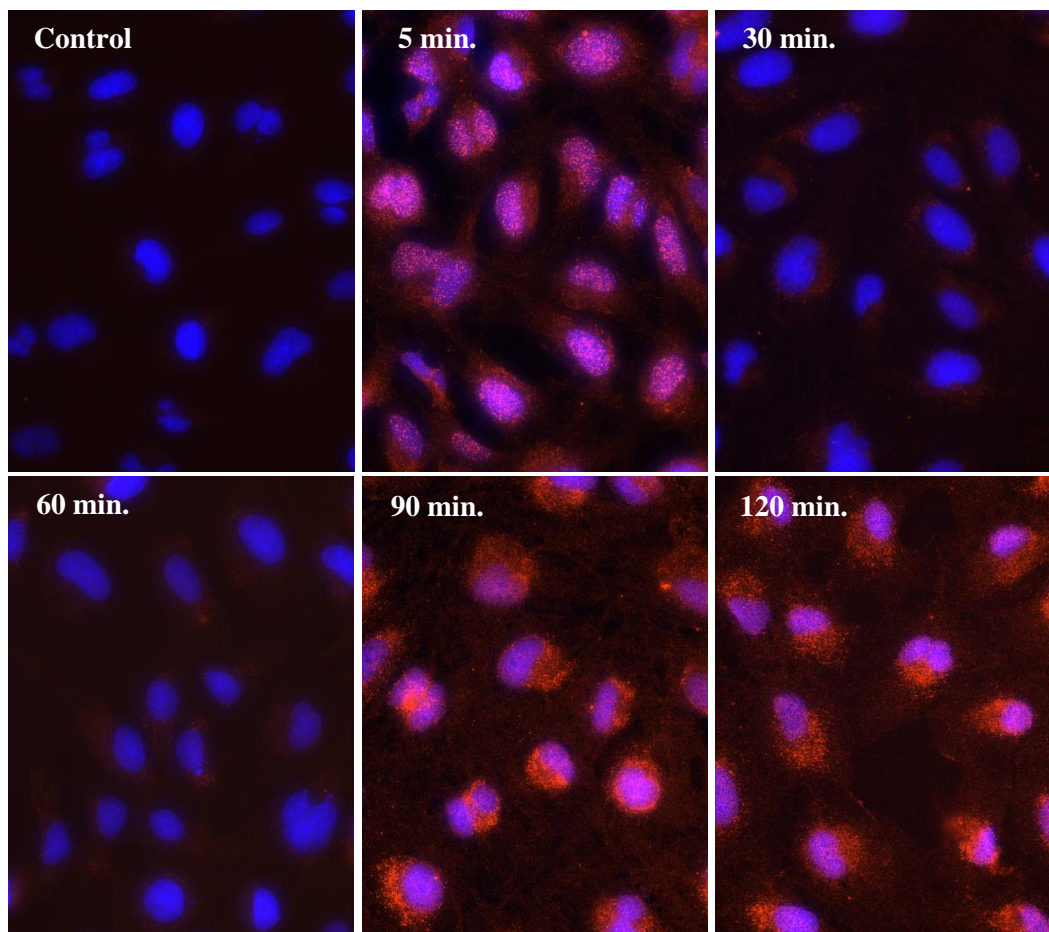


Figure 10: PAR staining in irradiated LECs after various incubation times. Blue= DAPI nuclei staining Red= PAR in cytoplasm Violet= PAR in nucleus.

Looking closely at the 5 minute and 90 minute time points, it was discovered that PAR is localized in different regions of the cell. Further magnification shows that after 5 minutes of incubation, about 80% of PAR exists in the nucleus while after 90 minutes PAR has moved with

80% now being present in the cytoplasm (Figure 11). It appeared that at 90 minutes, PAR poured out of the nucleus and entered the mitochondria.

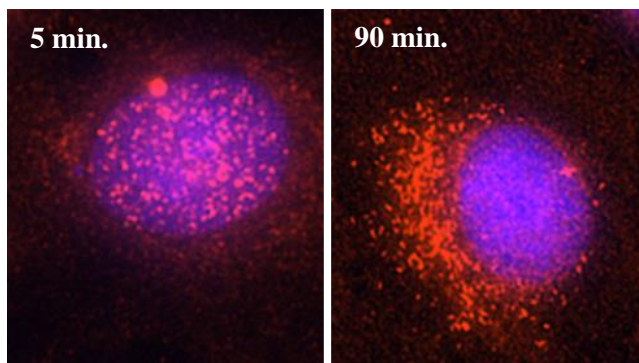


Figure 11: Closer look at localization of PAR in LECs 5 minutes and 90 minutes after UVB exposure. Note PAR is in the nucleus at 5 minutes (left) and then moves out into the cytoplasm, possibly into the mitochondria, at 90 minutes (right).

Immunocytochemistry: AIF

As mentioned previously, apoptosis inducing factor (AIF) was believed to be activated in response to the accumulation of PAR polymers in the mitochondria (Fatokun et al., 2014). Since PAR was observed flowing out of the nucleus into the mitochondria 90 minutes after UVB treatment (Fig. 11), we therefore thought that AIF was the missing link between DNA repair and eventual apoptosis. This, however, was not confirmed by AIF staining in LECs (Fig. 12). Expression of AIF is relatively constant at all time points after UVB exposure as well as in the absence of UVB with the control. It is also localized entirely in the mitochondria and is not seen in the nucleus. The parthanatos mechanism was not true for our particular cells.

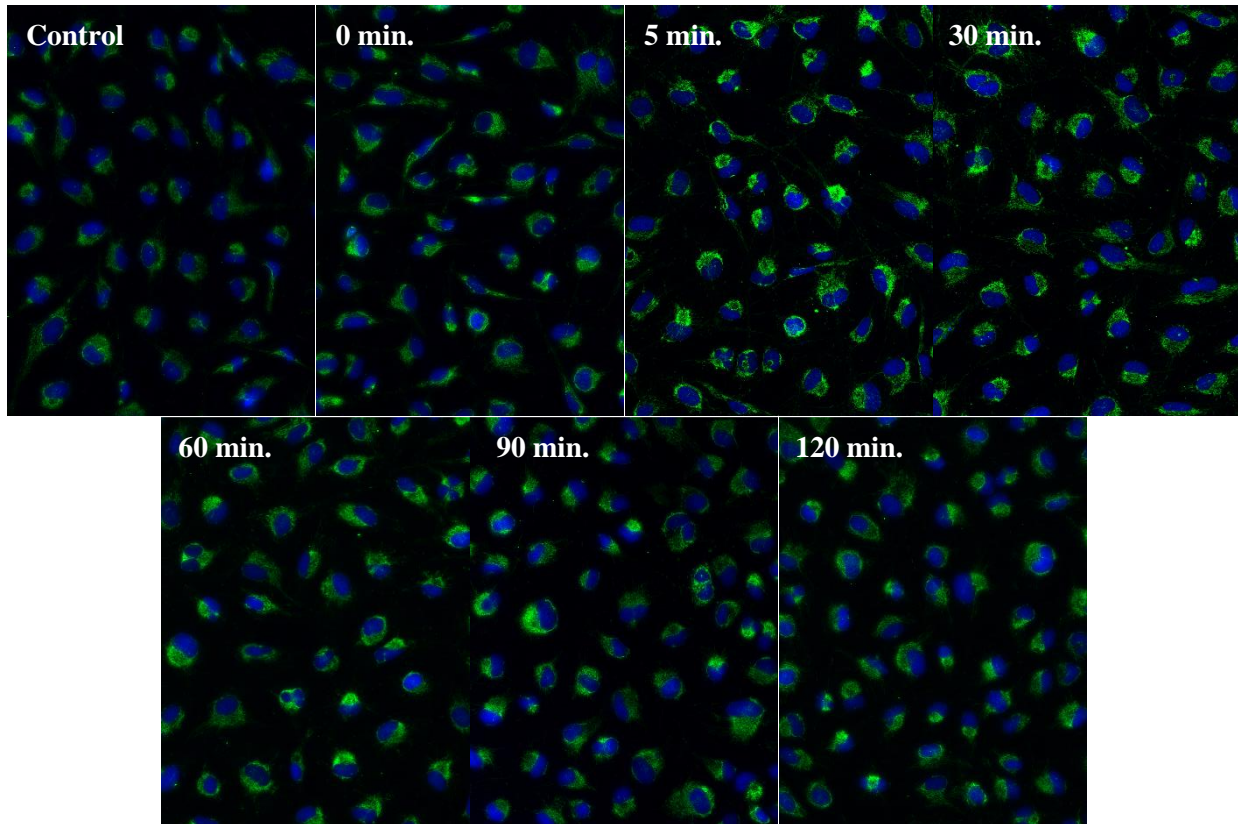


Figure 12: Apoptosis inducing factor staining in irradiated LECs following various incubation times. Blue= DAPI nuclei staining Green= AIF in mitochondria.

Discussion

We have shown that UVB causes visible morphological damage to LECs and dramatically affects their normal growth (Fig. 3). The exact type of damage being done involves UVB-induced single strand DNA breaks which leads to the fragmentation of DNA. To further examine the idea of cell damage in response to UVB radiation, we explored the topic of cell viability through the MTT assay. Figure 4 and Table 1 demonstrate the percentage of LECs lost over time. After UVB treatment, both 1 hour and 3 hour time points showed 26% and 28% cell loss, respectively. However, after 24 hours and 48 hours the decrease in the amount of viable cells appeared to be dramatic. One day after initial UVB exposure, 70% of LECs had died while 2 days after 80% had died. This supports the claim that UVB radiation causes significant cell

damage and death overtime due to DNA damage and cellular breakdown. Our $0.9\text{mW}/\text{cm}^2$ lethal dose of UVB light compares to physiological UVB exposure by being equivalent to about 36 hours of sunlight (Zigman, 1995). Although this seems like an extreme comparison, incoming UVB light is actually 20x as concentrated when entering the corners of the eyes describing a phenomenon known as the Coroneo effect (Coroneo, 2011). When the LECs first come into contact with UVB and absorb its harmful waves, they are instantly damaged and their DNA is broken. However, after 30 minutes of incubation the DNA has been repaired. This can be concluded from the comet assay images (Fig. 5) which initially show large comet tails followed by intact nuclei. Surprisingly, a second peak of DNA damage occurs 90 minutes after initial UVB exposure which leads into the topic of LECs having a biphasic damage and repair mechanism in response to UVB radiation.

Additionally, the DNA strand breaks were labeled with a TUNEL assay which tagged apoptosis generated breaks. This allowed for the discrimination of apoptosis, programmed cell death, from necrosis. We hypothesized that our cells would go toward apoptosis during times of the greatest cellular damage. If our hypothesis was correct, the apoptosis would be targeted at both 5 minutes and 90 minutes which were the two damage peaks seen in the comet assay. After experimentation and analysis (Fig. 6), it became apparent that apoptosis does follow the same biphasic pattern of damage that is seen in the comet assay.

Further testing for reactive oxygen species (ROS), H_2O_2 and superoxide anion, revealed the same biphasic pattern of cell damage as both the comet assay and the TMR Red kit. Since ROS can cause further DNA damage due to their potential destructive reactivity, it makes sense that these data match previous DNA fragmentation and cell death images. Experimentation revealed the presence of H_2O_2 in the nucleus (green dye) and cytoplasm (red dye) mostly at 90

minutes and 120 minutes after UVB exposure (Fig. 7). Time points before 90 minutes had a very low expression of ROS suggesting that the H₂O₂ takes time to develop in LECs after initial irradiation. Additionally, staining for superoxide anion shows that it does not develop in the mitochondria (red dye) until 90 minutes after UVB exposure (Fig. 8). Both of these sets of images support the deduction that the second peak of damage seen in the comet assay at 90 minutes is a result of ROS that have developed over time and cause indirect damage to LEC DNA.

In order to connect the entire story of UVB damage in LECs to the PARP-1/PAR repair mechanism, immunocytochemistry analysis was done. We started with PARP-1 in order to see if it is activated to repair DNA at only certain times after UVB exposure. The results revealed PARP-1 to be ever present in LEC nuclei regardless of UVB treatment and incubation time (Fig. 9). Therefore, if PARP-1 is constantly expressed we explored the hypothesis that it must be the presence of PAR that is changing in the mechanism. Interestingly, PAR expression follows the biphasic pattern of DNA damage (Fig. 10). Furthermore, fluorescent imaging showed that the localization of PAR moves from the nucleus, after 5 minutes, out into the cytoplasm, after 90 minutes (Fig. 11). We concluded that PARP-1 first detects DNA damage in the cell and then facilitates the formation of PAR and its recruitment into the nucleus (Fig. 13). PAR then helps repair the damage alongside PARP-1 and eventually moves into the cytoplasmic space.

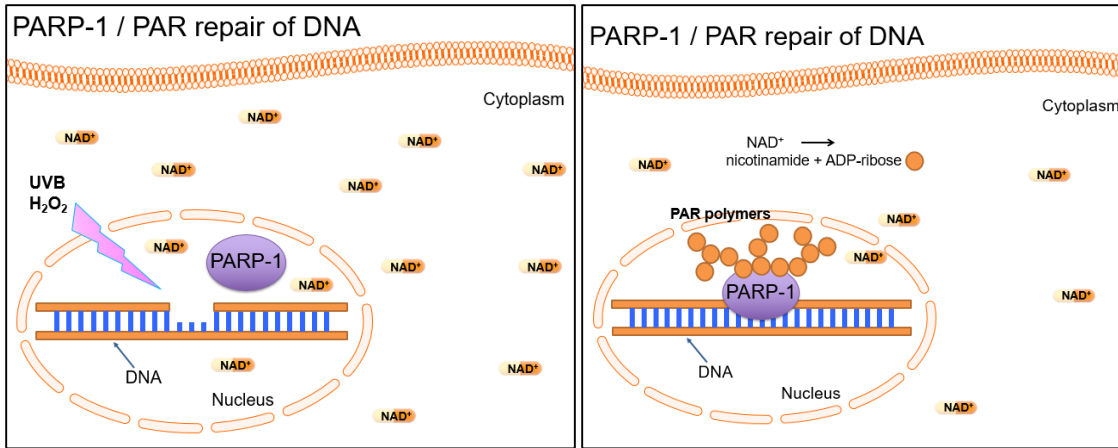


Figure 13: UVB-induced damage causes a single strand break in DNA. PARP-1 attaches to the area and recruits NAD⁺ in the cytoplasm to break up into nicotinamide and ADP-ribose. Poly(ADP-ribose) polymers (PAR) then move into the nucleus and repair DNA alongside PARP-1.

Localization of PAR at 5 minutes and 90 minutes is a key point to the mechanism. With the observed accumulation of PAR at 90 minutes in the cytoplasm, we believed it possible that it was in the mitochondria. Previous research has shown that PARP-1 and PAR can lead to parthanatos, a type of cell death caused by the overactivation of PARP-1 and the accumulation of PAR in the mitochondria (Fatokun et al., 2014). We therefore hypothesized that decreased cell viability seen overtime with the MTT assay could be caused by the parthanatos mechanism. After immunocytochemistry specific for AIF, however, we found that this was not the case. AIF is simply present in the mitochondria of the LECs all of the time in both the presence and absence of UVB (Fig. 12). In light of these results, the next step is to look into other ways that PAR could lead to cell death and apoptosis.

Conclusion

In conclusion, UVB radiation causes DNA damage in cultured human LECs. The resulting damage triggers PARP-1, which resides in the nucleus, to recruit the formation of PAR polymers to aid in DNA repair. If PARP-1 is over activated, however, an increased production of

PAR might turn the cell toward apoptosis and result in cell death over time. This could happen if levels of NAD⁺ became severely depleted, resulting in inhibition of the glycolytic pathway and low levels of ATP. The exact mechanism for apoptosis is still being explored. Future plans for this project include research on PAR causing apoptosis in addition to testing inhibitors for PARP-1 to see what will happen when UVB-induced damage occurs in the absence of PARP-1 facilitated repair. We may also wish to measure levels of NAD⁺ and ATP in the cells to better understand the mechanism.

Works Cited

- Coroneo, M. (2011). Ultraviolet radiation and the anterior eye. *Eye & Contact Lens*, 37(4), 214-224. doi:10.1097/ICL.0b013e318223394e
- Fatokun, A., Dawson, V., & Dawson, T. (2014). Parthanatos: Mitochondrial-linked mechanisms and therapeutic opportunities. *British Journal of Pharmacology*, 171(8), 2000-2016. doi:10.1111/bph.12416
- Ibaraki, N., Chen, S., Lin, L., Okamoto, H., Pipas, J., & Reddy, V. (1998). Human lens epithelial cell line. *Experimental Eye Research*, 67(5), 577-85.
- Jaffe, N., & Horwitz, J. (1992). In Steven M. Podos, Myron Yanoff (Ed.), *Lens and cataract* (3rd ed.). New York: Gower Medical Publishing.
- Li, W., Kuszak, J., Dunn, K., Wang, R., Ma, W., Wang, G., . . . Weiss, M. (1995). Lens epithelial cell apoptosis appears to be a common cellular basis for non-congenital cataract development in humans and animals. *The Journal of Cell Biology*, 130(1), 169-181. doi:10.1083/jcb.130.1.169
- Luo, X., & Kraus, W. (2012). On PAR with PARP: Cellular stress signaling through poly(ADP-ribose) and PARP-1. *Genes and Development*, 26(5), 417-432. doi:10.1101/gad.183509.111
- Murphy, M. (2008). How mitochondria produce reactive oxygen species. *Biochemical Journal*, 417(1), 1-13. doi:10.1042/BJ20081386

Riss, T., Moravec, R., Niles, A., Benink, H., Worzella, T., & Minor, L. (2013). Cell viability assays. In G. Sittampalam, N. Coussens & H. Nelson (Eds.), *Assay guidance manual* () Eli Lilly & Company and the National Center for Advancing Translational Sciences.

Taylor, H., West, S., Rosenthal, F., Muñoz, B., Newland, H., Abbey, H., & Emmett, E. (1988). Effect of ultraviolet radiation on cataract formation. *The New England Journal of Medicine*, 319(22), 1429-1433. doi:10.1056/NEJM198812013192201

Zigman, S. (1995). Environmental near-UV radiation and cataracts. *Optometry and Vision Science*, 72(12), 899-901.